In-Plane and Out-of-Plane Infrared Difference Spectroscopy Unravels Tilting of Helices and Structural Changes in a Membrane Protein upon Substrate Binding

ARTICLE *in* JOURNAL OF THE AMERICAN CHEMICAL SOCIETY · OCTOBER 2009

Impact Factor: 12.11 · DOI: 10.1021/ja906324z · Source: PubMed

J|A|C|S COMMUNICATIONS

Published on Web 10/05/2009

In-Plane and Out-of-Plane Infrared Difference Spectroscopy Unravels Tilting of Helices and Structural Changes in a Membrane Protein upon Substrate Binding

Víctor A. Lórenz-Fonfría,*,† Meritxell Granell,† Xavier León,†,§ Gérard Leblanc,‡ and Esteve Padrós†

Unitat de Biofísica, Departament de Bioquímica i de Biologia Molecular, and Centre d'Estudis en Biofísica, Universitat Autònoma de Barcelona, 08193 Bellaterra, Barcelona, Spain, and Institut de Biologie et Technologies-Saclay, Service de Bioenergétique, Biologie Structurale et Mécanismes, CEA-Saclay, F-91191 Gif sur Yvette, France

Received July 28, 2009; E-mail: victor.lorenz@gmail.com

The characterization of conformational changes triggered by the interaction of substrates/ligands with membrane proteins is an essential step toward understanding both molecule transport and signal transduction in cells. A steadily growing number of X-ray crystallographic atomic models of secondary transporters hold promise for revealing the structural basis of their transport mechanisms.[1] To date, however, only for lactose permease have X-ray structures been solved for both ligand-free and ligand-bound forms.[2] They reveal few structural changes localized in the binding pocket, which contrasts with the results of studies under more functional conditions that suggest major changes in the tilt of helices upon lactose binding.[3] This example highlights the need for structural methods alternative to X-ray crystallography that are able to assay substrate-induced changes under conditions as physiological as possible, ideally without using potentially perturbing probes. Here we present a spectroscopic approach fulfilling these requirements that is based on a change of coordinates allowing the computation of infrared (IR) difference spectra in and out of the plane of an attenuated total reflection (ATR) crystal from polarized data. Spectroscopic rules for unequivocally discriminating between changes in the tilt of transmembrane helices and other structural rearrangements are also introduced. We have applied the present method to characterize the structural changes in the secondary transporter melibiose permease (MelB) from *Escherichia coli* driven by the binding and transport of the disaccharide melibiose.

IR difference spectroscopy stands out because of its ability to monitor changes in protein backbone and amino acid side chains in membrane proteins in a preserved lipid environment without the need for external probes.[4] Near-physiological conditions in terms of hydration, ionic strength, and temperature can be attained in the ATR mode, where precise control of the buffer medium is trivial. In IR difference spectroscopy, a reconstituted membrane protein is switched between two states (e.g., from **A** to **B**) by either light, an electrochemical potential, or (as done here) alternation of buffers without and with substrates. An IR difference spectrum is obtained and corrected for all nonspecific changes.[5] Negative and positive peaks emerge as a result of changes in the frequency and/or intensity of the transition dipole moments, **M**, of the different vibrations in going from **A** to **B**. This is caused either by chemical changes (e.g., deprotonation of a carboxylic group), environment changes (e.g., a change in the H-bonding strength), or conformational changes (e.g., a change in the vibrational coupling of the peptide bond), providing the grounds for the interpretation of IR difference spectra in structural terms.[4]

The stacked disposition of the sample in the ATR crystal plane (*x*,*y* in Figure 1) makes ATR-IR difference spectra also sensitive to changes in the orientation of **M** with respect to the ATR surface normal (the *z* direction) even when unpolarized IR light is used.[6] However, this sensitivity is habitually insufficient for beneficial use but can be intense enough to complicate the interpretation of the difference spectra. As simulated in Figure 1 for a Ge crystal, both the protonation of a carboxylic group (Figure 1a) and its reorientation (Figure 1b) give rise to positive bands in unpolarized difference spectra, although the latter is much less intense [but see Figure S1 in the Supporting Information (SI) for a different ATR crystal]. Equivalently, both the elongation of a helix (Figure 1c) and a decrease in its tilt (Figure 1d) give rise to positive bands at the amide I vibration frequency expected for transmembrane helices. The behavior of the amide II vibration is more complex as a result of two orthogonal split modes (A and E_1).

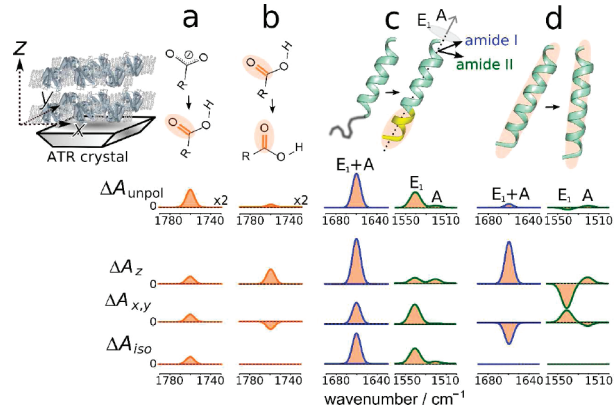

Figure 1. Schematic representation of the origins of bands in IR difference spectra of axially distributed reconstituted protein samples: (a) deprotonation and (b) reorientation of one carboxylic group; (c) elongation and (d) reorientation of one helix. The displayed intensities for ΔA_{unpol} correspond to unpolarized light with a Ge crystal ($n_1 \approx 4$). The bottom part shows the corresponding ΔA_z, $\Delta A_{x,y}$, and ΔA_{iso} values. Negative bands from the lost carboxylate group in (a) and from the lost loop structure in (c) have been omitted for clarity. For further details, see the SI.

Through the use of parallel and perpendicular polarized light, nonisotropic samples with axial symmetry can be appropriately characterized.[7] However, it has been shown that substrate-induced polarized difference spectra, $\Delta A_{||}$ and $\Delta A_{\perp}$, are difficult to interpret.[8] In contrast, difference spectra along the *z* axis and in the *x*,*y* plane would allow for a more straightforward structural interpretation. The different behavior of ΔA_z and $\Delta A_{x,y}$ allow the discrimination of bands originating from changes in vibration frequencies (or intensities), characterized by identical signs for ΔA_z and $\Delta A_{x,y}$ (Figure 1a,c), from those arising from pure reorientation changes, which have opposite signs for ΔA_z and $\Delta A_{x,y}$ (Figure 1b,d). Furthermore, the isotropic difference spectrum (Figure 1), which is free from reorientation-related effects, can then be easily computed as $\Delta A_{iso} = \Delta A_z + 2\Delta A_{x,y}$.[6] In contrast, the use of ΔA_{unpol}, or even $\Delta A_{||}$ and $\Delta A_{\perp}$, leads to mixed bands coming from both reorientation and environmental changes.

As described in a different context,[6] in an ATR setup, ΔA_z and $\Delta A_{x,y}$ can be obtained by combination of $\Delta A_{||}$ and $\Delta A_{\perp}$ as follows:

† Universitat Autònoma de Barcelona.
‡ Institut de Biologie et Technologies-Saclay.
§ Present address: Centre de Biotecnologia Animal i Teràpia Gènica, Universitat Autònoma de Barcelona.

10.1021/ja906324z CCC: $40.75

$$\Delta A_{x,y} = \Delta A_{\perp}/E_y^{\,2}$$

$$\Delta A_z = (\Delta A_{||} - \Delta A_{\perp}E_x^{\,2}/E_y^{\,2})/E_z^{\,2} \qquad (1)$$

where $\mathbf{E} = (E_x, E_y, E_z)$ is the electric field vector of the ATR evanescent wave normalized to the incident wave, computed here using the thick-film hypothesis.[9] Equation 1 was further modified to take into account the polarizer leak fraction (see the SI).

We applied these concepts to the substrate-induced IR difference spectra of MelB, a membrane protein that is able to couple the active transport of melibiose to the electrochemical gradient of each of three different cations (H^+, Na^+, or Li^+).[10] The MelB was purified and reconstituted in *E. coli* lipids as described elsewhere.[5] Figure 2a shows difference spectra induced by melibiose in the presence of Na^+ obtained by repetitively cycling buffers without and with melibiose[5] and alternating parallel- and perpendicular-polarized light during the acquisition (see Figure S3).

The computed ΔA_z and $\Delta A_{x,y}$ are shown in Figure 2b (original spectra), and their uncertainties are displayed in Figure S2. We will focus the discussion on the amide I bands, which are more informative and straightforward to interpret than the amide II bands. The most remarkable feature is the opposite sign of ΔA_z and $\Delta A_{x,y}$ at ~1665−1655 cm^{-1}, with ΔA_{iso} close to zero at ~1658 cm^{-1} (Figure 2b original), suggesting from the wavenumber and the intensity pattern the reorientation of some transmembrane helices (compare with Figure 1d left). However, the band broadening intrinsic to IR spectroscopy precludes a clear resolution of the component bands.

We applied a maximum-entropy deconvolution method[11] to mathematically reduce the width of the bands in the difference spectra (Figure 2b, narrowed spectra). After this, a completely resolved peak at 1658 cm^{-1} appeared in both ΔA_z and $\Delta A_{x,y}$ (red dashed box in Figure 2b), and its assignment to a reduced tilt of some helices became clear, as it fulfilled the intensity pattern for ΔA_z, $\Delta A_{x,y}$, and ΔA_{iso} shown in Figure 1d. This same band was previously resolved as a positive peak[5] (i.e., reorientation of groups contributes to the unpolarized difference absorbance), as we illustrated in Figure 1.

Interestingly, the peak at 1658 cm^{-1} was recently found to be absent in a mutant that binds but does not transport melibiose,[12] clearly suggesting that the detected helix tilt is associated not with the sugar-binding process but with the following sugar/cation cotransport. The observed reduction of the tilt of some helices of MelB most likely reflects the formation of the so-called occluded state (Figure 2b inset), one of the proposed intermediate states by which secondary transporters may alternate access to the substrate binding site from either side of the membrane.[1]

We should also note that the same sign is observed in both ΔA_z and $\Delta A_{x,y}$ for the rest of the bands in the amide I region (~1700−1620 cm^{-1}). The same holds for the bands in the amide II region (~1580−1510 cm^{-1}), which reports more averaged structural changes because of its lower structure sensitivity. The detected decrease in the tilt of some helices should therefore be accompanied by an important structural reorganization (e.g., elongation/disruption of helices/loops). For instance, the positive peak at 1667 cm^{-1} shows higher intensity in ΔA_z than in $\Delta A_{x,y}$ and is likely to originate from the elongation of some transmembrane helices with low tilt upon melibiose binding, in accordance with Figure 1c.

In summary, the study and interpretation of the structural changes in membrane proteins upon substrate binding is simplified by computing ΔA_z, $\Delta A_{x,y}$, and ΔA_{iso} from polarized IR difference spectra. In combination with simple rules and band-narrowing methods, it can allow structural and orientation changes induced by substrate binding to be disentangled. Further structural and functional insights are possible if this method is combined with site-directed mutagenesis or isotopic labeling. The present approach can be also useful in the structural interpretation of light- and potential-induced IR difference spectra of proteins.

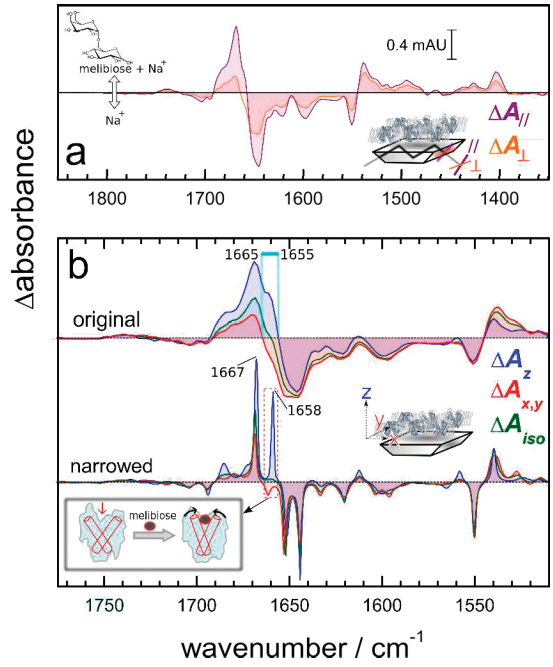

Figure 2. (a) Melibiose-induced polarized IR difference spectra of MelB reconstituted in *E. coli* lipids in the presence of Na^+ [10 mM NaCl, 100 mM KCl, 20 mM MES (pH 6.6)] using 10 mM melibiose. Difference spectra were obtained with a KRS polarizer at 4 cm^{-1} resolution with 16 000 averaged scans each. (b) Calculated difference spectra along the z axis (blue) and in the x,y plane (red) obtained as $\Delta A_z = 0.410\Delta A_{||} - 0.360\Delta A_{\perp}$ and $\Delta A_{x,y} = 0.454\Delta A_{\perp} - 0.011\Delta A_{||}$, respectively. The original difference spectra were mathematically narrowed as described in ref 5. The calculated ΔA_{iso} spectrum is shown in green. The inset shows the molecular interpretation of the intensity pattern of the band at ~1658 cm^{-1}.

Acknowledgment. This work was supported by UAB Postdoctoral Fellowship 40607 and Marie Curie Reintegration Grant PIRG03-6A-2008-231063 (to V.A.L.-F.) and by Dirección General de Investigación Grant BFU2006-04656/BMC (to E.P.).

Supporting Information Available: Figures S1−S3 and methods for computing the intensities in Figure 1 and estimating ΔA_z and $\Delta A_{x,y}$ from $\Delta A_{||}$ and $\Delta A_{\perp}$, taking into account the polarizer leak. This material is available free of charge via the Internet at http://pubs.acs.org.

References

(1) DeFelice, L. J. *Trends Neurosci.* **2004**, *27*, 352. Karpowich, N. K.; Wang, D. N. *Science* **2008**, *321*, 781. Diallinas, G. *Science* **2008**, *322*, 1644.
(2) Abramson, J.; Smirnova, I.; Kasho, V.; Verner, G.; Kaback, H. R.; Iwata, S. *Science* **2003**, *301*, 610. Mirza, O.; Guan, L.; Verner, G.; Iwata, S.; Kaback, H. R. *EMBO J.* **2006**, *25*, 1177.
(3) Smirnova, I.; Kasho, V.; Choe, J. Y.; Altenbach, C.; Hubbell, W. L.; Kaback, H. R. *Proc. Natl. Acad. Sci. U.S.A.* **2007**, *104*, 16504. Zhou, Y.; Guan, L.; Freites, J. A.; Kaback, H. R. *Proc. Natl. Acad. Sci. U.S.A.* **2008**, *105*, 3774.
(4) Nyquist, R. M.; Ataka, K.; Heberle, J. *ChemBioChem* **2004**, *5*, 431. Rich, P. R.; Iwaki, M. *Mol. BioSyst.* **2007**, *3*, 398. Barth, A.; Zscherp, C. *Q. Rev. Biophys.* **2002**, *35*, 369.
(5) León, X.; Lórenz-Fonfría, V. A.; Lemonnier, R.; Leblanc, G.; Padrós, E. *Biochemistry* **2005**, *44*, 3506.
(6) Marsh, D. *Biophys. J.* **1999**, *77*, 2630.
(7) Fraser, R. D. B. *J. Chem. Phys.* **1953**, *21*, 1511.
(8) Hill, D. G.; Baenziger, J. E. *Biophys. J.* **2006**, *91*, 705.
(9) Goormaghtigh, E.; Raussens, V.; Ruysschaert, J. M. *Biochim. Biophys. Acta* **1999**, *1422*, 105.
(10) Pourcher, T.; Bassilana, M.; Sarkar, H. K.; Kaback, H. R.; Leblanc, G. *Philos. Trans. R. Soc. London, Ser. B* **1990**, *326*, 411. Ganea, C.; Fendler, K. *Biochim. Biophys. Acta* **2009**, *1787*, 706.
(11) Lórenz-Fonfría, V. A.; Padrós, E. *Appl. Spectrosc.* **2005**, *59*, 474.
(12) León, X.; Leblanc, G.; Padrós, E. *Biophys. J.* **2009**, *96*, 4877.

JA906324Z

Supporting information to: In-plane and out-of-plane infrared difference spectroscopy unravels helices tilt and structural changes in a membrane protein upon substrate binding

Víctor A. Lórenz-Fonfría,[*,†] Meritxell Granell,[†] Xavier León,[†] Gérard Leblanc,[‡] and Esteve Padrós[†]

Unitat de Biofísica, Departament de Bioquímica i de Biologia Molecular, and Centre d'Estudis en Biofísica, Universitat Autònoma de Barcelona, 08193 Bellaterra, Barcelona, Spain; and Institut de Biologie et Technologies-Saclay, Service de Bioenergétique, Biologie Structurale et Mécanismes. CEA-Saclay, F-91191 Gif sur Yvette, France

E-mail: victor.lorenz@gmail.com

Supporting Methods

Computation of ΔA_{unpol}, ΔA_z, $\Delta A_{x,y}$ and ΔA_z in the simulations. In a Fourier transform IR spectrophotometer the IR beam has no significant preferential polarization (1). As a consequence the absorbance measured without polarizer is given by: $A_{unpol} \approx (A_{//} + A_{\perp})/2$, where $A_{//}$ and $A_{\perp}$ are the absorbance than would be measured with light parallel and perpendicular polarized to respect the plane of incidence, respectively (see for instance Fig. 1 in ref. 2). In an ATR experiment with perfectly perpendicular and parallel polarized light, $A_{//}$ and $A_{\perp}$ are given by: $A_{\perp} = k\langle M_y^2\rangle E_y^2$ and $A_{//} = k(\langle M_x^2\rangle E_x^2 + \langle M_z^2\rangle E_z^2)$, where k is a proportionality constant and $\langle\ \rangle$ stands for time and space average (2). $\mathbf{M} = (M_x, M_y, M_z)$ is the transition dipole moment of a given vibration, and $\mathbf{E} = (E_x, E_y, E_z)$ is the electric field vector of the ATR evanescent wave normalized to the electric field vector of the incident wave, where z is the direction perpendicular to the ATR crystal plane, and x and y are two perpendicular directions laying in the ATR crystal plane (see figures 2b in the paper or Fig. 1 in ref. 2). Taking into account the axial symmetry of the sample along the z axis we have: $\langle M_x^2\rangle = \langle M_y^2\rangle = |\mathbf{M}|^2\times\langle\sin^2\varphi\rangle/2 = |\mathbf{M}|^2\times\langle 1 - \cos^2\varphi\rangle/2$, and $\langle M_z^2\rangle = |\mathbf{M}|^2\times\langle\cos^2\varphi\rangle$, where φ is the angle made by $\mathbf{M}$ with the z axis. Combining the above equations we arrive to an expression that approximately describes the absorbance in ATR with unpolarized light:

$$A_{unpol} = k|\mathbf{M}|^2 \times \left(\frac{\langle\cos^2\varphi\rangle E_z^2}{2} + \frac{\langle\sin^2\varphi\rangle\left(E_x^2 + E_y^2\right)}{4} \right) \qquad \text{(S1)}$$

Equation S1 can be more conveniently expressed using the order parameter S_φ:

$$A_{unpol} = k|\mathbf{M}|^2 \times \left(\frac{3E_z^2}{2\left(2S_\varphi + 1\right)} + \frac{3E_x^2 + E_y^2}{4\left(1 - S_\varphi\right)} \right) \qquad \text{(S2)}$$

where $S_\varphi = (3\langle\cos^2\varphi\rangle - 1)/2$. Substituting for E_x, E_y, and E_z analytical expressions derived from the "weak absorber thick film" approximation (3), and simplifying:

$$A_{unpol} = k|\mathbf{M}|^2 \times \left(\frac{2n_1^2\cos^2\theta\left\{\left[3n_1^2 + n_2^2 - \left(1 - S_\varphi\right)\right]\sin^2\theta + 2n_2^2\left(S_\varphi - 1\right)\right\}}{3\left(n_1^2 - n_2^2\right)\left[\left(n_1^2 + n_2^2\right)\sin^2\theta - n_2^2\right]} \right) \qquad \text{(S3)}$$

where n_1 is the refraction index of the crystal (e.g., $n_1 \approx 4.0$ for Ge, $n_1 \approx 3.42$ for Si, and $n_1 \approx 2.4$ for ZnS, ZnSe and diamond), n_2 is the refraction index of the sample (e.g., $n_2 \approx 1.32$ for water, $n_2 \approx 1.45$ for dry lipids, and $n_2 \approx 1.7$ for dry proteins), and θ is the angle of incidence of the IR beam in the ATR crystal surface with the z axis (3). For calculating the relative intensities show in Fig. 1 we used $n_1 \approx 4.0$ (Ge crystal), $n_2 \approx 1.4$, and $\theta = 45^o$:

$$A_{unpol} = k|\mathbf{M}|^2 \times (1.140 + 0.159 S_\varphi) \quad \text{(S4)}$$

and for computing the data in Fig. S1 n_1 was changed to 2.4 (i.e., ZnS, ZnSe or diamond crystal):

$$A_{unpol} = k|\mathbf{M}|^2 \times (1.516 + 0.782 S_\varphi) \quad \text{(S5)}$$

From eq. S3-S5 we can calculate how a change of $k|\mathbf{M}|^2$ or a change of S_φ will change A_{unpol}. Note also that Eq. S4-S5 clearly shows that as n_1 becomes smaller the contribution of changes of S_φ to changes in A_{unpol} will be larger (compare eq. S4 and S5, and Fig. 1 and Fig. S1). The value of $k|\mathbf{M}|^2$ was arbitrarily taken as 1 for the amide I vibration (for one peptide bond) and for the C=O vibration of one carboxylic group. For the amide II vibration, $k|\mathbf{M}|^2$ was taken as 0.45 for the E_1 mode and 0.05 for the A mode, which are in agreement with known values of absorption coefficient of these vibrations in relative terms (4). For the computation of ΔA_{unpol} in case of the helices we took into account that $S_\varphi = S_\beta S_\alpha$, where β is the tilt angle of the helix axis to respect the z axis, and α is the angle of the amide I transition dipole moment to respect the helix axis ($S_\alpha \approx 0.43$) (4). For the amide II, $S_\alpha = -0.5$ for the E_1 mode and $S_\alpha = 1$ for the A mode (4).

For A_z and $A_{x,y}$:

$$A_{//} = k|\mathbf{M}|^2 \langle \cos^2 \varphi \rangle = k|\mathbf{M}|^2 \left(\frac{2S_\varphi + 1}{3} \right) \quad \text{(S6)}$$

$$A_{\perp} = k|\mathbf{M}|^2 \left(\frac{1 - \langle \cos^2 \varphi \rangle}{2} \right) = k|\mathbf{M}|^2 \left(\frac{1 - S_\varphi}{3} \right) \quad \text{(S7)}$$

which were used to compute ΔA_z and $\Delta A_{x,y}$ from changes of $k|\mathbf{M}|^2$ and S_φ. Finally, ΔA_{iso} was calculated as $(\Delta A_z + 2\Delta A_{x,y})/3$, which taking into account Eq. S6-S7 reduces to: $\Delta A_{iso} = \Delta(k|\mathbf{M}|^2)/3$. Note that ΔA_{iso} is not sensitive to changes in the orientation of $\mathbf{M}$, since it does not depend on S_φ.

Estimation of ΔA_z, $\Delta A_{x,y}$ and ΔA_{iso} from experimental $\Delta A_\perp$ and $\Delta A_{//}$ taking into account the polarizer leak. The projected absorbance into the z axis and the x,y plane can be obtained as: $A_{x,y} = A_\perp / E_y^2$ and $A_z = (A_{//} - A_\perp E_x^2 / E_y^2) / E_z^2$, as shown in ref. 2. Equivalent expressions apply to compute $\Delta A_{x,y}$ and ΔA_z from $\Delta A_\perp$ and $\Delta A_{//}$. To calculate E_x^2, E_y^2 and E_z^2 we used the weak absorber thick film approximation. The applicability of the "thick film" approximation follows from the amount of proteoliposomes deposited over the ATR crystal (see below), and it is further warranted by the presence of buffer (bulk water) over the sample. There is also evidence that the "weak absorber" approximation is reasonably accurate, even for strong absorbing bands, provided that the wavenumber-dependence of n_2 (anomalous dispersion) is taken into account (5, 6). In the computation of E_x^2, E_y^2 and E_z^2 we took into account our experimental optical conditions, assigning some reasonable uncertainties expressed as plus/minus two standard deviations: $n_1 = 4.0 \pm 0.01$ and $\theta = 45 \pm 2^o$. To estimate n_2 in our sample, we toke into account that the concentration of water in the sample area sensed by the evanescent wave was estimated to be ~880 mg/ml (i.e, 120 mg/ml of proteoliposomes), and so $n_2 \approx 1.32 \times 0.88 + 1.55 \times 0.12 \approx 1.35 \pm 0.05$. This leads to the following expressions to calculate the absorbance in the z and x-y directions from polarized difference absorbance spectra: $\Delta A_{x,y} =$

$(0.443\pm0.032)\times\Delta A_{\perp}$ and $\Delta A_z = (0.393\pm0.036)\times\Delta A_{//} - (0.342\pm0.033)\times\Delta A_{\perp}$, where the errors correspond to plus/minus two standard deviations estimated using Monte Carlo method using 10^4 random samples. We should note, however, that this computation of $\Delta A_{x,y}$ and ΔA_z and their uncertainties assumes that n_2 is wavenumber-independent, a convenient and extensively used approximation (3), but not fully accurate.

The above derivation ignores that polarizers are not perfect, having some fraction leak, f (7). Considering f to be small, the absorbance difference with perpendicular and parallel polarized light can be expressed as: $\Delta A_{\perp} = (1-f)\times\Delta A_{\perp}^{ideal} + f\times\Delta A_{//}^{ideal}$, and $\Delta A_{//} = (1-f)\times \Delta A_{//}^{\text{ideal}} + f\times\Delta A_{\perp}^{\text{ideal}}$. Substituting and solving for $\Delta A_{x,y}$ and ΔA_z:

$$\Delta A_{x,y} = \frac{\Delta A_{\perp}(1-f) - \Delta A_{//} f}{E_y^2(1-2f)} \tag{S8}$$

$$\Delta A_z = \frac{\Delta A_{//}\left(E_y^2(1-f) + E_x^2 f\right) - \Delta A_{\perp}\left(E_x^2(1-f) + E_y^2 f\right)}{E_y^2 E_z^2(1-2f)} \tag{S9}$$

The value of f was estimated to be ~ 0.039 for the polarizer used in this work. This value was estimated as before (8). Briefly, for a substance without a preferential orientation (e.g., a liquid) deposited over an ATR crystal with θ=45°, the isotropic ratio (i.e., the ratio making $A_{//} \approx R^{iso} A_{\perp}$) should be exactly 2, but will decrease as f increases. This allows estimating f from the experimental value of R^{iso} as:

$$f = \frac{\left(R^{iso}-2\right)\left(n_2^2 - n_1^2\right)}{R^{iso}\left(n_1^2 - n_2^2\right) + n_2^2} \tag{S10}$$

or in case θ is not exactly 45° as:

$$f = \frac{n_2^2\left(R^{iso}-1\right) - \left[R^{iso}\left(n_2^2 + n_1^2\right) - 2n_1^2\right]\sin^2\theta}{\left[R^{iso}\left(n_1^2 - n_2^2\right) - n_2^2\right]\sin^2\theta + n_2^2} \tag{S11}$$

In our experimental setup we obtained $R^{iso} \approx 1.92\pm0.03$ for pure liquid water, from where we deduced from Eq. S11 that $f \approx 0.039\pm0.017$, where the error comes from the uncertainties in n_1, n_2, θ and R^{iso}. Then, applying Eq. S8-S9 we arrive to: $\Delta A_{x,y} = (0.454\pm0.031)\times\Delta A_{\perp} - (0.011\pm0.009)\times\Delta A_{//}$ and $\Delta A_z = (0.410\pm0.036)\times\Delta A_{//} - (0.360\pm0.034)\times\Delta A_{\perp}$. The isotropic difference absorbance is then obtained as $\Delta A_{iso} = (\Delta A_z + 2\Delta A_{x,y}) / 3 \approx (0.129\pm0.013)\times\Delta A_{//} + (0.184\pm0.010)\times\Delta A_{\perp}$. As we show in Fig. S2a, the effect of the experimental uncertainties in n_1, n_2, θ and f on the estimation of $\Delta A_{x,y}$, ΔA_z and ΔA_{iso} are rather small, with few spectra changes mostly reduced to intensity differences. These small visual differences are even reduced after mathematically band-narrowing (Fig. S2b), attesting for the robustness of the introduced method to uncertainties in the computation of the evanescent electromagnetic fields and the polarizer leak. Nevertheless, we should note that the computation of $\Delta A_{x,y}$ and specially ΔA_z involves the subtraction of two difference spectra, and therefore the signal-to-noise ratio will be reduced after this transformation of coordinates..

Sample preparation and data acquisition. MelB expression, purification and reconstitution into liposomes were carried out as described (9). Sample preparation for ATR-IR difference spectra was done basically as before (10). An aliquot of ~20 µl of proteoliposomes containing about 150 µg of MelB was spread homogeneously on a germanium ATR crystal (50×10×2 mm, Harrick, Ossining, NY, yielding 12 internal

reflections at the sample side) and dried gently at room humidity. The sample was rehydrated with buffer **A** (10 mM NaCl, 100 mM KCl, 20 mM MES at pH 6.6). After equilibration for the film swelling the exchange of buffers (without and with melibiose) and the collection of polarized IR spectra started, using the protocol shown in Fig. S3. Spectra were recorded with a FTS6000 Bio-Rad spectrometer, equipped with a mercury-cadmium-telluride detector. Sample temperature was adjusted to 20.0 ^{o}C using a cover jack placed over the ATR crystal connected to a circulating thermostatic bath. The cover jack temperature was controlled with a fitted external probe.

References

1. Sperline, R. P. (1991) *Appl. Spectrosc.* **45,** 677-81.
2. Marsh, D. (1999) *Biophys. J.* **77,** 2630-7.
3. Goormaghtigh, E., Raussens, V. & Ruysschaert, J. M. (1999) *Biochim. Biophys. Acta* **1422,** 105-85.
4. Marsh, D., Müller, M. & Schmitt, F. J. (2000) *Biophys. J.* **78,** 2499-510.
5. Max, J.-J. & Chapados, C. (1999) *Appl. Spectrosc.* **53,** 1045-1053.
6. Averett, L. A., Griffiths, P. R. & Nishikida, K. (2008) *Anal. Chem.* **80,** 3045-9.
7. Myers, C. W. & Cooper, S. L. (1994) *Appl. Spectrosc.* **48,** 72-78.
8. Dave, N., Lórenz-Fonfría, V. A., Leblanc, G. & Padrós, E. (2008) *Biophys. J.* **94,** 3659-70.
9. Dave, N., Lórenz-Fonfría, V. A., Villaverde, J., Lemonnier, R., Leblanc, G. & Padrós, E. (2002) *J. Biol. Chem.* **277,** 3380-7.
10. León, X., Lórenz-Fonfría, V. A., Lemonnier, R., Leblanc, G. & Padrós, E. (2005) *Biochemistry* **44,** 3506-14.

Supporting Figures

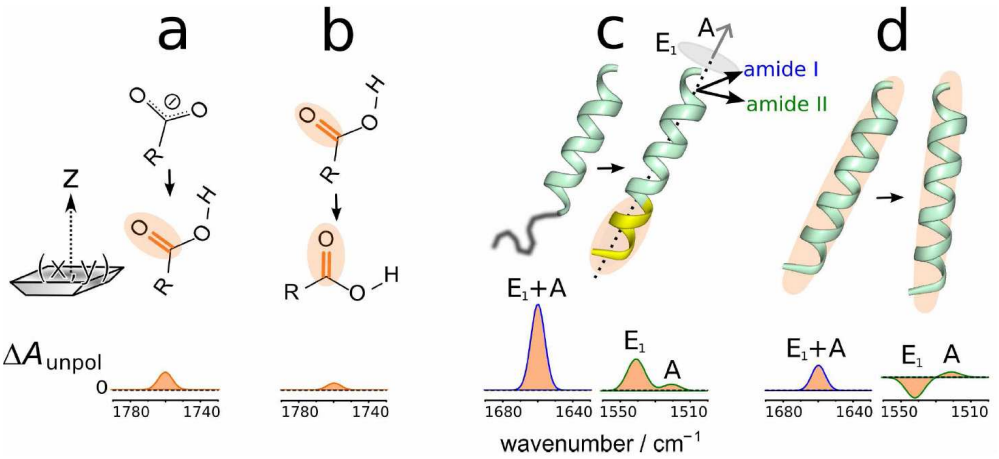

Figure S1. Origins of bands in IR difference spectra of non-isotropic samples: (a) deprotonation and (b) reorientation of one carboxylic group; and (c) grow and (d) reorientation of one helix. The displayed intensities for ΔA_{unpol} correspond to unpolarized light with an ATR crystal with $n_1 \approx 2.4$ (ZnSe, ZnS, or diamond).

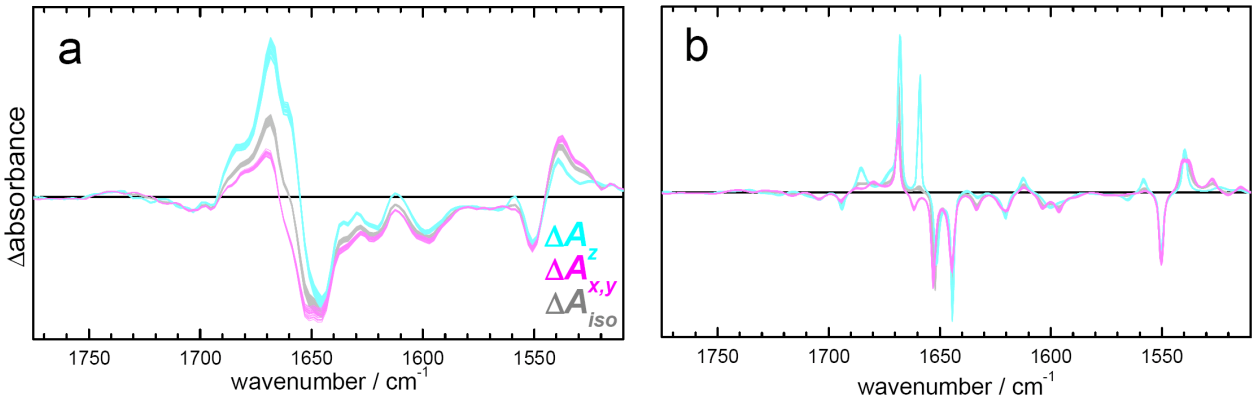

Figure S2. In-plane, out-of-plane and isotropic IR difference spectra, taking into account the uncertainties in the evaluation of the evanescent electric magnetic field and the polarizer leak fraction. Twenty possible outputs are shown. (a) Original difference spectra. (b) Band-narrowed difference spectra.

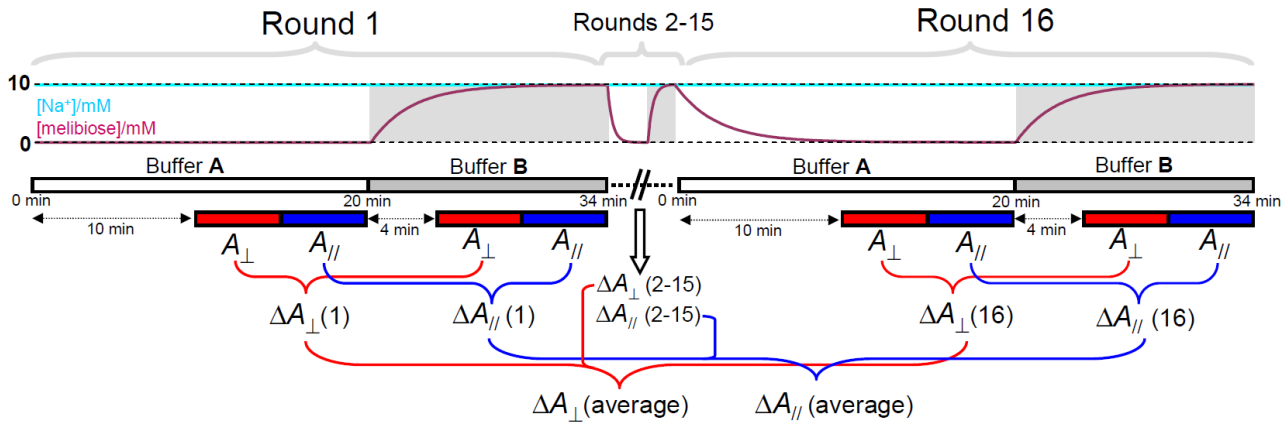

Figure S3. Scheme of the data acquisition protocol. Buffers **A** (white box) and **B** (gray box) are alternatively passed through the ATR sample compartment at a flow of ~1.5 ml/min until completing 16 rounds (~9 hours). Buffer **A** (10 mM NaCl, 100 mM KCl, 20 mM MES at pH 6.6) reduces the concentration of melibiose in the sample compartment to zero, while buffer **B** (buffer **A** with 10 mM melibiose) increases it to ~10 mM (see purple concentration profile). The sodium concentration is keep to ~10 mM during the whole experiment (see cyan concentration profile). Absorbance spectra are recorded during the last 10 min of buffers **A** or **B** perfusion, first using perpendicular polarized light (red box), and then using parallel polarized light (blue box), averaging 1000 interferograms at 4 cm^{-1} resolution for each condition. Melibiose-induced difference spectra are computed for each round. After manual inspection, the difference spectra obtained for the different rounds are averaged, and corrected for the melibiose absorbance and sample swelling as described before (10). In the last round the intensities of $\Delta A_{\perp}$ and $\Delta A_{//}$ were still ~85% of the intensities in the first round, assessing for the preserved sample integrity during the measurements. Note than the average concentration of melibiose during the acquisition of $\Delta A_{\perp}$ will be slightly lower than during the acquisition of $\Delta A_{//}$ for buffer **B**, and slightly higher for buffer **A**, which may lead to intensity differences. The same experiment was conducted with unpolarized light, and we confirmed that the first difference spectrum was slightly less intense (with an 88% intensity of the second one). Therefore, to compensate for this effect, the obtained $\Delta A_{\perp}$(average) was multiplied by 0.88^{-1}.